## FEATURES

- Stable and reliable in performances
- Compact size
- RoHS compliant

RoHS Compliant
includes all homogeneous materials
(see part numbering system for details)

## APPLICATIONS

- ISM 868/915 Bands
- Smart meters
- Wireless alarm and security system
- Industrial monitoring and control
- IOT applications

## SPECIFICATIONS

| | |
|---|---|
| **Electrical** | |
| Frequency Range | 863 ~ 873 MHz<br>910 ~ 920 MHz |
| Center Frequency | 868 MHz<br>915 MHz |
| Polarization | Linear |
| Impedance | 50Ω |
| **Dimensions (mm):** | |
| Body Length (A) | 35 ± 2.0 |
| Width (C) | 7.0 ± 1.0 |
| Cable Length (B) | 38 ± 5.0 |
| Cable Type | RF1.13 |
| Connector Type | IPEX (MHF I) |

NAN-F 868-915 DB - 105 X 38 A F
- F = RoHS compliant
- A = RF1.13 Cable
- 38 = Cable length in mm
- X = IPEX Connector
- 105 = Version Code (See page 7)
- DB = Dual Band
- 868 – 915 = Center Frequency
- NAN-F = Series

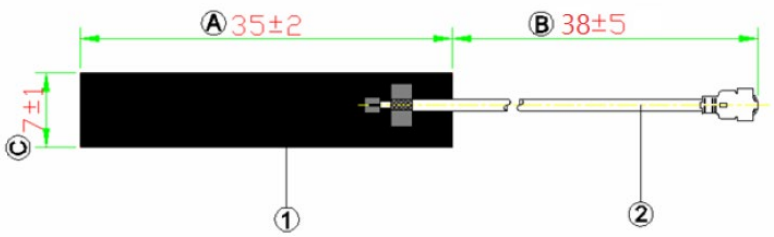


| Item | Name | Material | Color |
|---|---|---|---|
| 1 | NAN-F_FPC | PI | Black |
| 2 | I-PEX & RF1.13 | FEP | Gray |

**Setup:**

**S-Parameters (Impedance, Return Loss, and VSWR)**

- Equipment - Network Analyzer (Agilent E5071A)

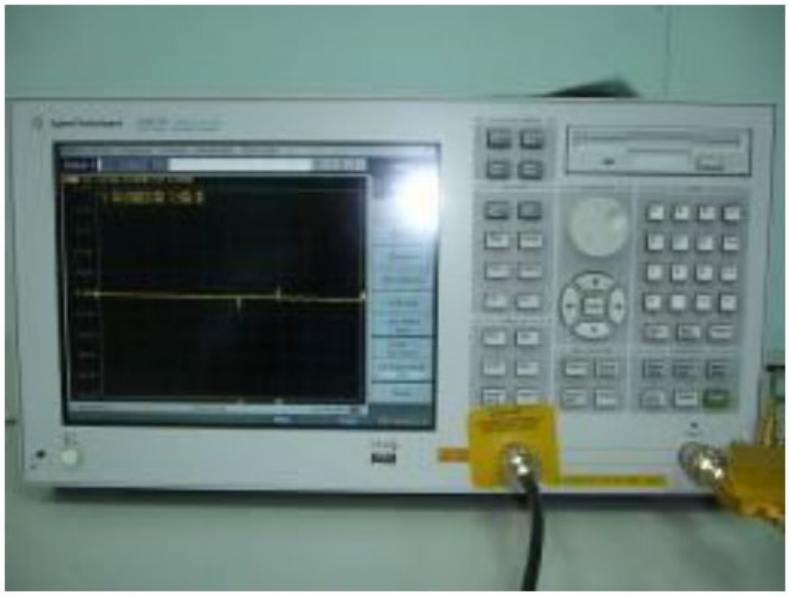

Figure. Network Analyzer(Agilent E5071A)

**Radiation Patterns ( Gain, Efficiency, 2D gain patterns and 3D gain Patterns)**

- Equipment- Anechoic Chamber, Network Analyzer (Agilent E5071C), Standard Horn.

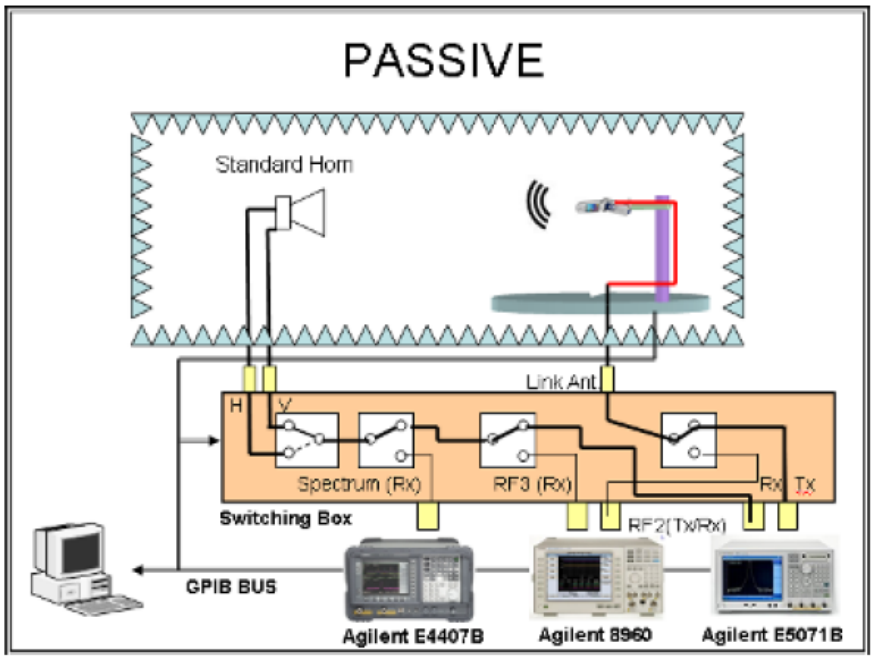


Figure. Scheme of radiation pattern measurement system

## Antenna Placement


## Return Loss

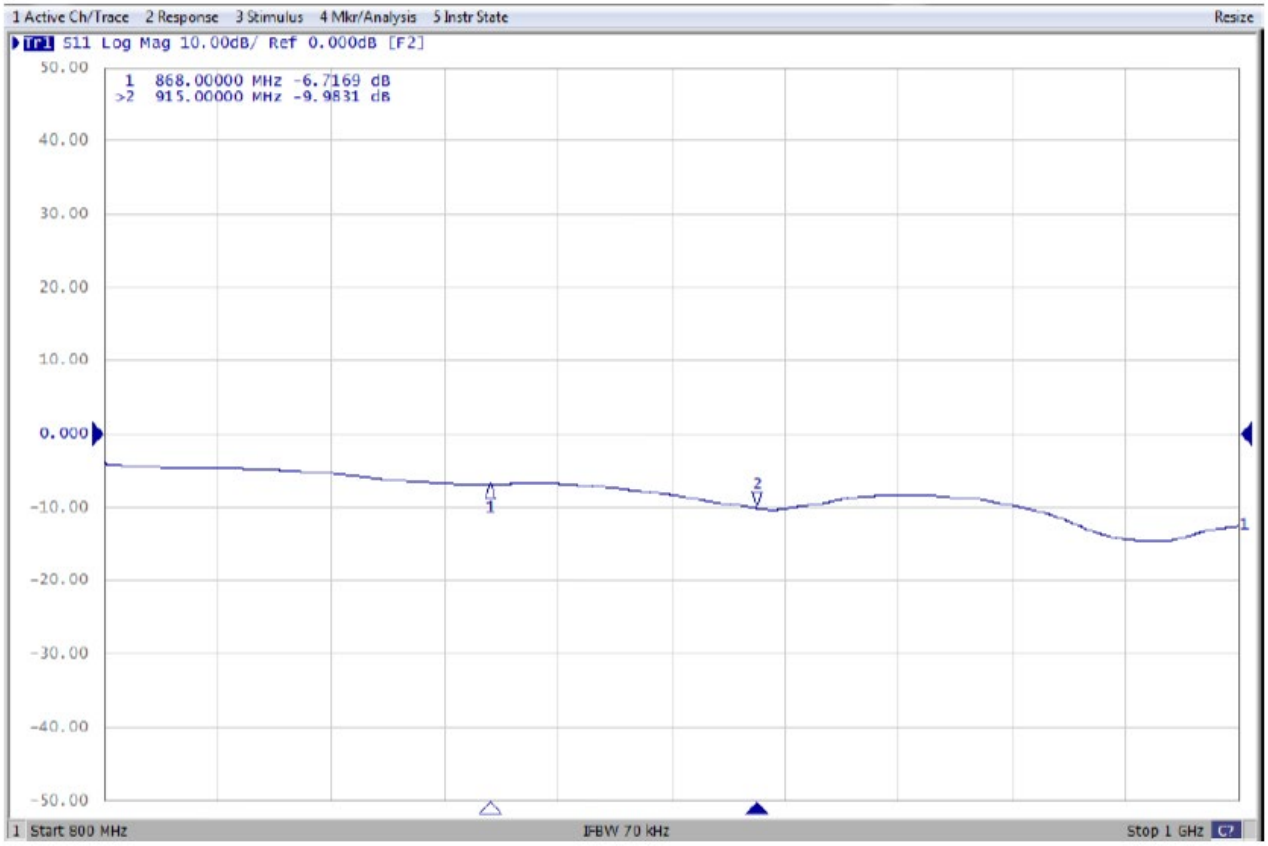

**Radiation Efficiency**

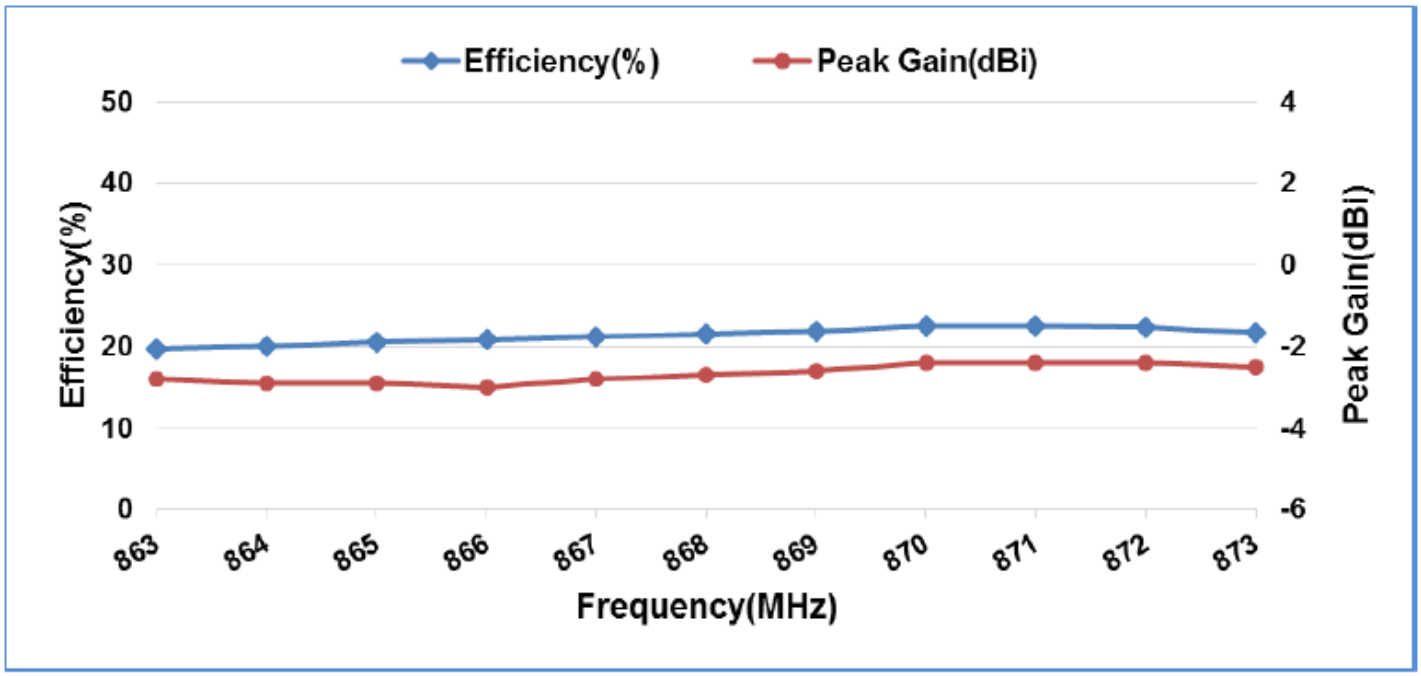


**863 ~ 873 MHz**

| Frequency (MHz) | 863 | 864 | 865 | 866 | 867 | 868 | 869 | 870 | 871 | 872 | 873 |
|---|---|---|---|---|---|---|---|---|---|---|---|
| Efficiency (dB) | -7.1 | -7.0 | -6.9 | -6.8 | -6.7 | -6.7 | -6.6 | -6.5 | -6.4 | -6.5 | -6.6 |
| Efficiency (%) | 19.6 | 20.0 | 20.5 | 20.8 | 21.2 | 21.6 | 21.9 | 22.5 | 22.6 | 22.3 | 21.7 |
| Peak Gain (dBi) | -2.8 | -2.9 | -2.9 | -3.0 | -2.8 | -2.7 | -2.6 | -2.4 | -2.4 | -2.4 | -2.5 |

**Radiation Efficiency**

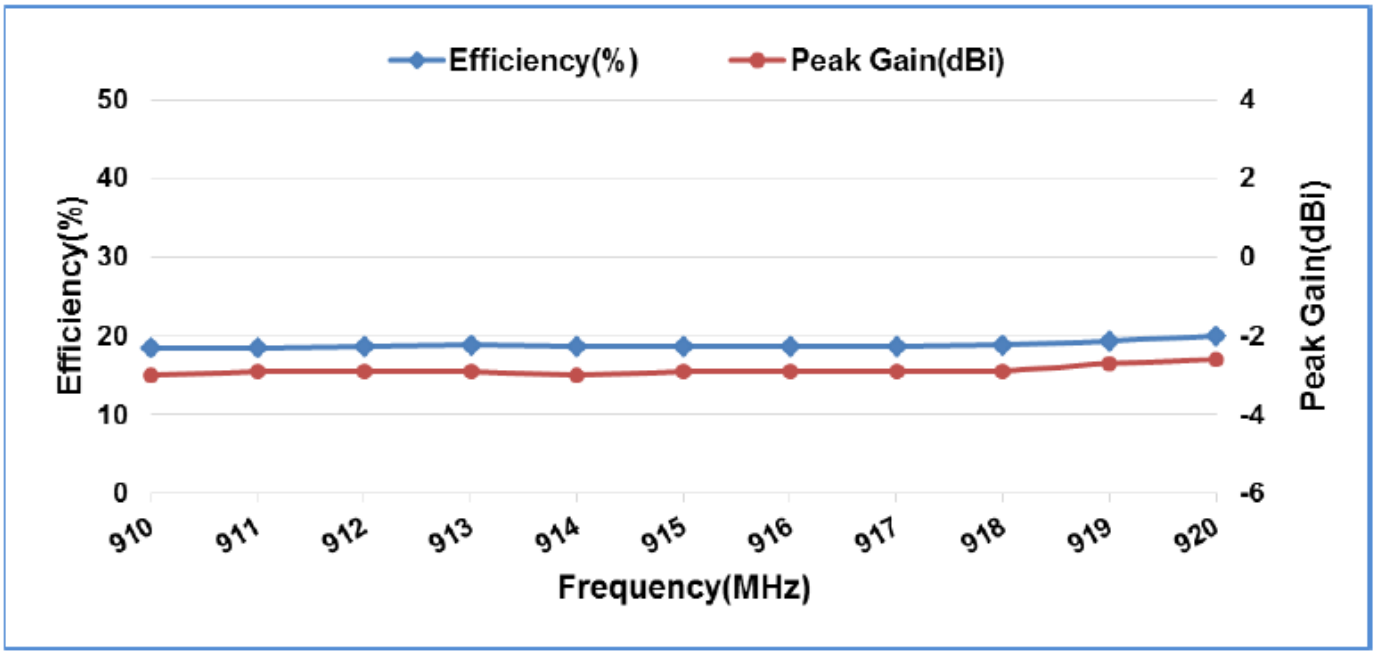


**910 ~ 920 MHz**

| Frequency (MHz) | 910 | 911 | 912 | 913 | 914 | 915 | 916 | 917 | 918 | 919 | 920 |
|---|---|---|---|---|---|---|---|---|---|---|---|
| Efficiency (dB) | -7.3 | -7.3 | -7.3 | -7.3 | -7.3 | -7.3 | -7.3 | -7.3 | -7.3 | -7.1 | -7.0 |
| Efficiency (%) | 18.5 | 18.5 | 18.7 | 18.8 | 18.7 | 18.7 | 18.7 | 18.6 | 18.8 | 19.4 | 20.0 |
| Peak Gain (dBi) | -3.0 | -2.9 | -2.9 | -2.9 | -3.0 | -2.9 | -2.9 | -2.9 | -2.9 | -2.7 | -2.6 |

## RADIATION PATTERNS

3D Gain Pattern ( Radiation Pattern @ 868 MHz) (unit: dBi)

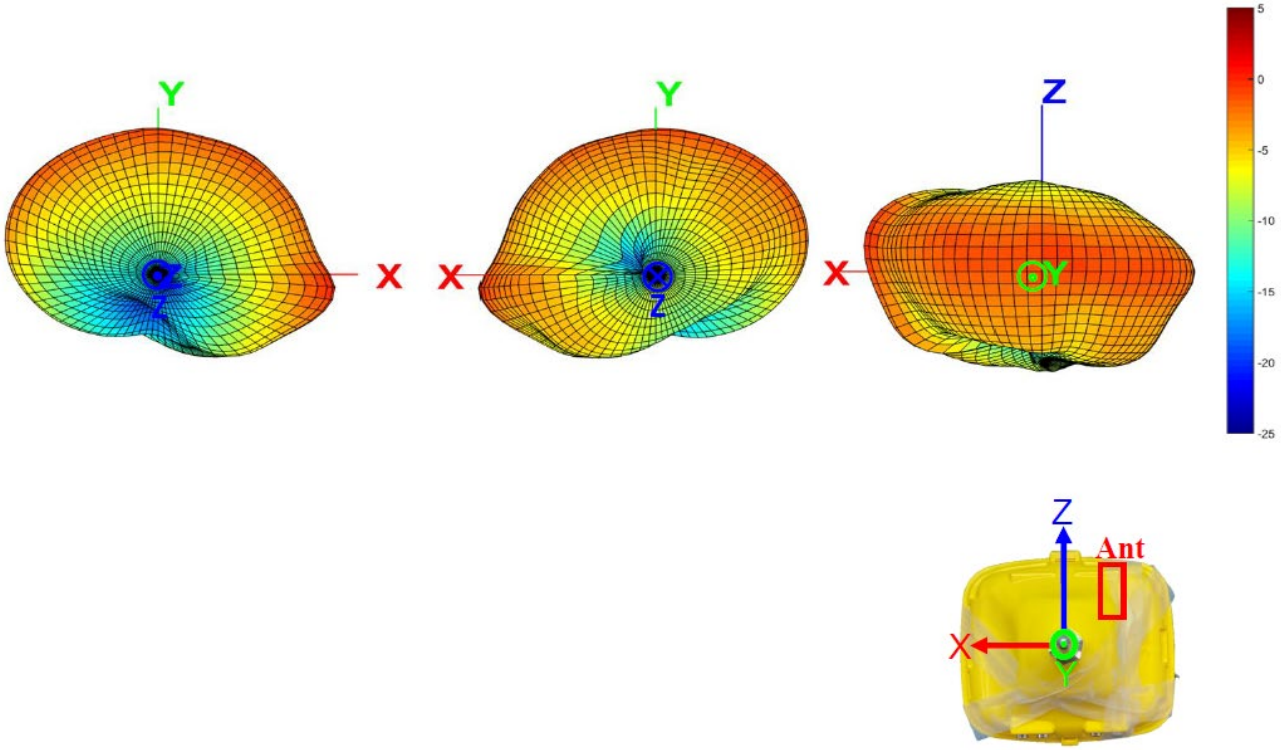


3D Gain Pattern ( Radiation Pattern @ 915 MHz) (unit: dBi)

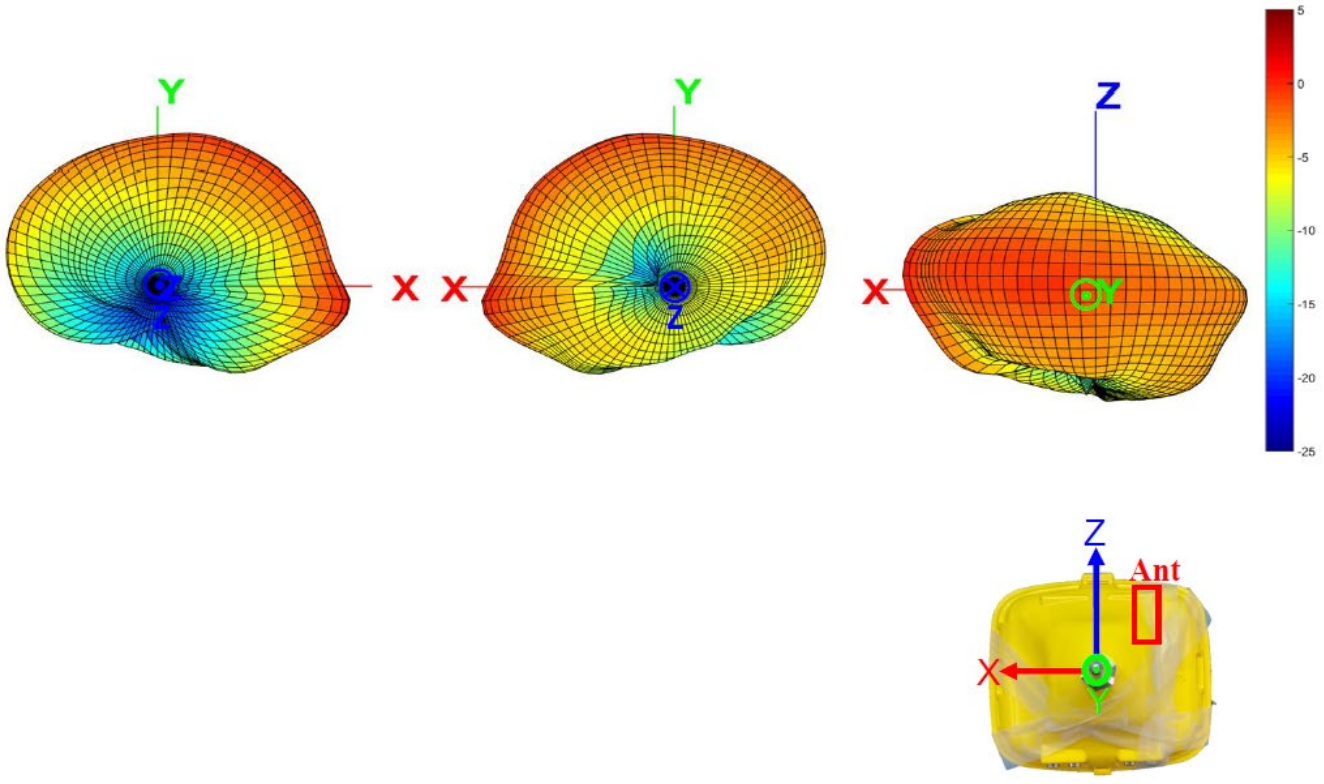

## Version History and Status

| Version | Date Issued | Details | Status |
|---|---|---|---|
| **105** | October 18th 2022 | **Initial Release**<br>Inova DOT Program | Supported |
| | | | |
| | | | |
| | | | |
| | | | |

**Please reach out to NIC for any customization requests and other inquiries:**

- NIC Technical Support: tpmg@niccomp.com
- Compliance Support: rohs@niccomp.com

# On-board antennas reference design for the STM32WB Series MCUs

## Introduction

This document describes the design, fabrication, and radio electrical characterization (S11 parameter and radiation) of a set of seven antennas associated with their electronic board, operating on the ISM 2.45 GHz frequency band and available for the STM32WB Series microcontrollers.

The seven antenna types are:

- Monopole T-shaped antenna
- Monopole L-shaped antenna
- Inverted F Antenna – IFA
- Microstrip meandered monopole antenna
- IFA metal plane antenna
- Yagi-Uda antenna
- Chip antenna

**Figure 17. Simulated radiation pattern for the simplified and complete models at 2.45 GHz: (a) φ=0° (XZ plane), (b) φ=90° (YZ plane), (c) Θ=90° (XY plane)**

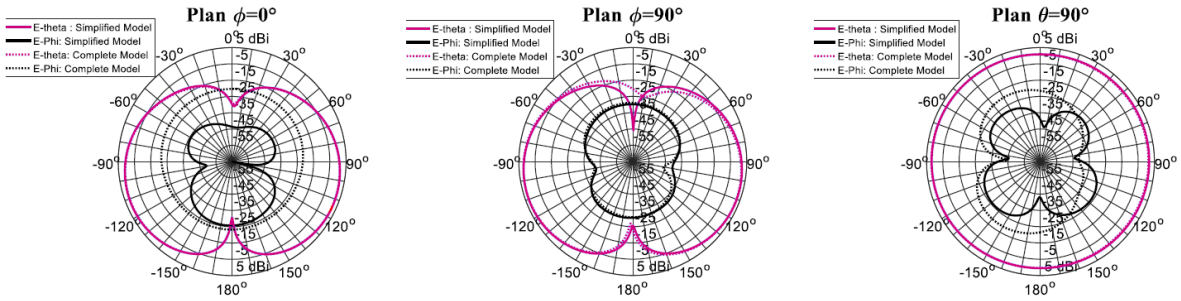


(a) (b) (c)

## 3.5 Inverted F antenna - IFA

### 3.5.1 Configuration

Numerous research studies are conducted to analyze the Inverted-F antenna such as in [4] where the authors present experimental observations about the IFA performances at the frequency 1.8 GHz for portable handsets.

The 3D inverted-F antenna is also explored in the presence of parasitic elements in 1989 by H.Nakano and his colleagues[5], to reveal the behavior of the input impedance and to widen the impedance bandwidth.

Similarly, the geometry and dimensions of the proposed inverted F antenna conceived here, are shown in Figure 18. The simplified and complete designs are also investigated here to ensure good accuracy results. This design is compact compared to the previous ones with an overall size of 52 x 30 $mm^2$. Additionally, to optimize the location of the radiating element on the small PCB, an L-shaped extension is added to achieve resonance at the desired frequency without increasing the PCB dimensions as presented in Figure 18 (a).

**Figure 18. Inverted-F antenna configuration: (a) simplified model (b) complete model**

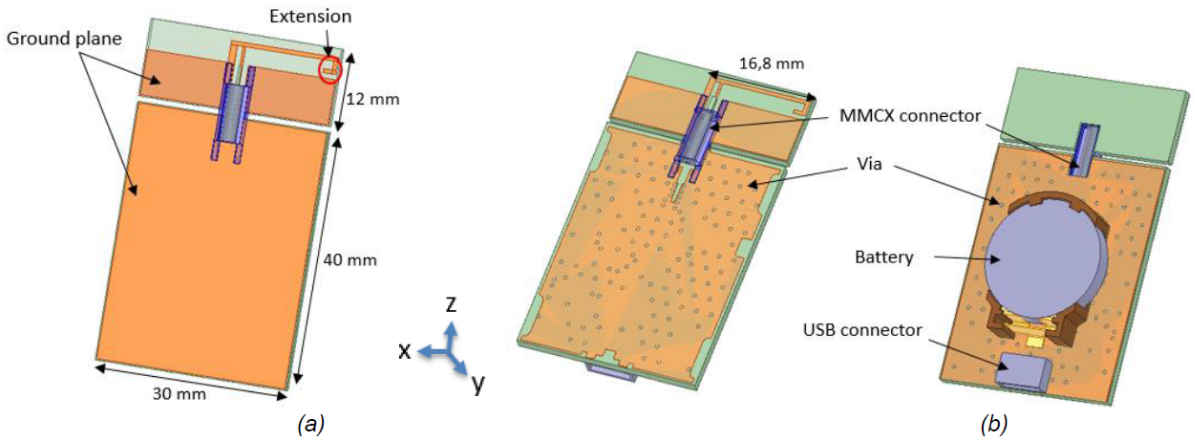


(a) (b)

### 3.5.2 Simulation results

The proposed IFA models are designed also on the FR4 substrate based on dimensions shown in Figure 18. The simulated return loss for the simplified model is shown as a black line, while the complete one is as a dashed red line in Figure 19. A slight shift of the resonance frequency can be observed when the antenna is placed on its real environment. However, a good reflection coefficient is maintained over the ISM range of frequencies. Notice that the resonance associated with the chip PCB is not excited with this compact antenna topology and the matching frequency band is consequently narrower.

In Figure 20, the simulated input impedance variation within frequency is exposed. An insignificant difference is observed in terms of real and imaginary parts when switching to a complete model.

**Figure 19. Simulated return loss versus frequency for simple and complete models**

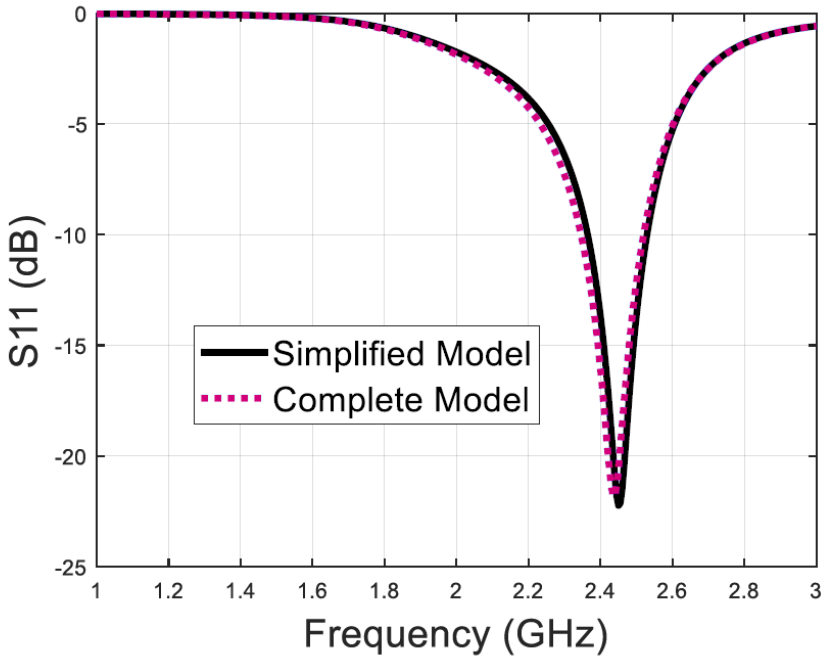


**Figure 20. Simulated input impedance versus frequency for simple and complete models**

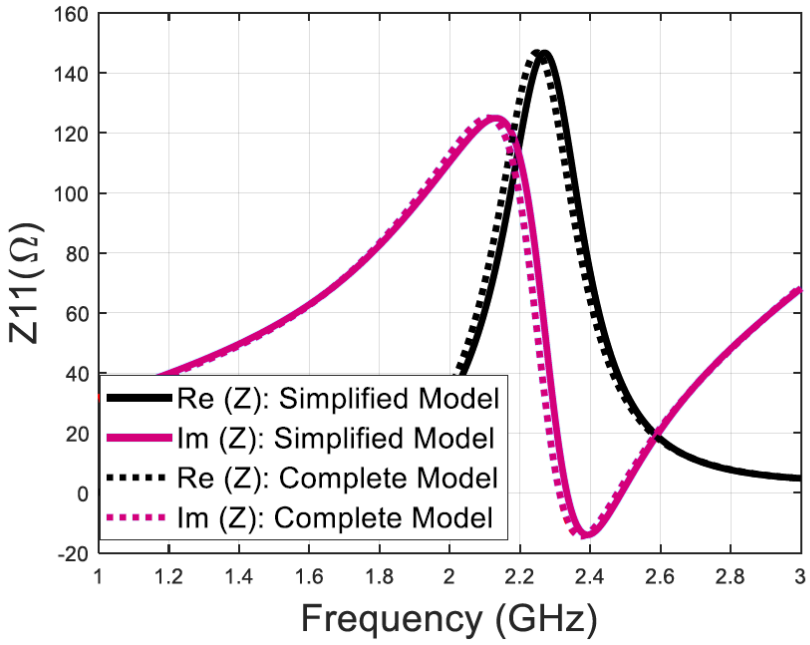

Figure 21 illustrates the total efficiency of the IFA antenna against frequency. A decrease of 1.6 % is observed in the case of the complete model compared to the simple one. Figure 22 shows the 2D radiation pattern in terms of gain, in three different planes at 2.45 GHz. Omnidirectional radiation is observed in the plane Θ=90°. Notice that a good agreement is achieved between the complete and simplified models, except the cross-polarization level that increases in the φ=0° and Θ=90°. The asymmetry of the diagram is observable in the φ=0° cut plane due to antenna topology.

**Figure 21. Simulated efficiency versus frequency for simple and complete models**

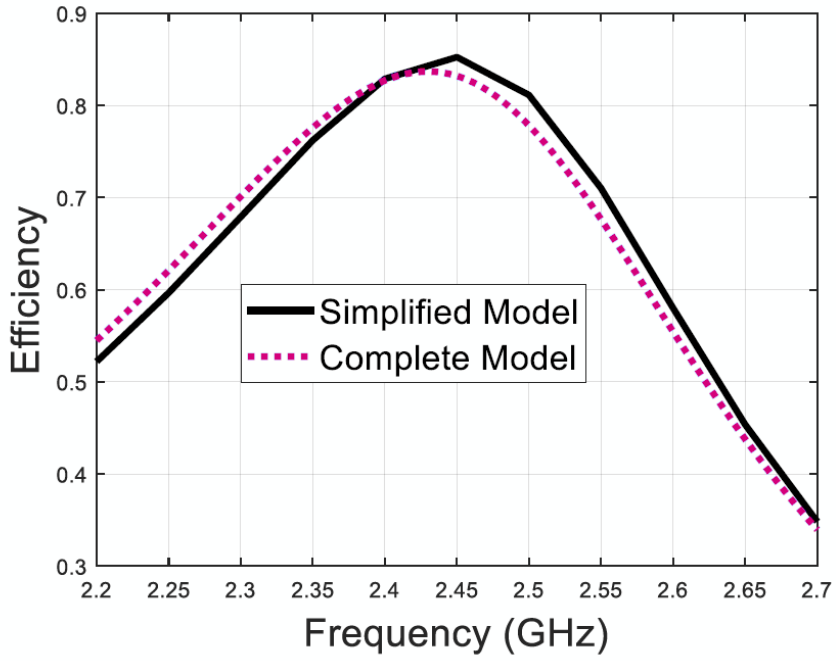


**Figure 22. Simulated radiation pattern for the simplified and complete models at 2.45 GHz: (a) φ=0° (XZ plane), (b) φ=90° (YZ plane), (c) Θ=90° (XY plane)**

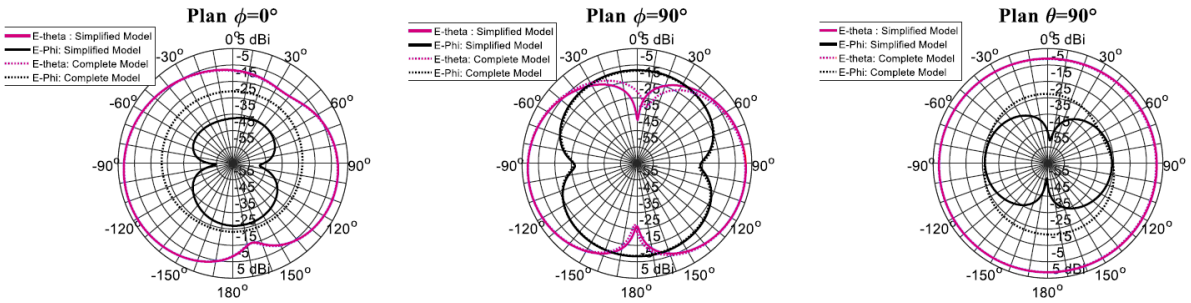


## 3.6 Metallic inverted F antenna

### 3.6.1 Configuration

The geometrical configuration of a simple Metallic Inverted F Antenna is studied as shown in Figure 23. It is soldered on the FR-4 substrate and consists of a bent monopole parallel to the PCB with a short circuit implemented arm. Basic and complete models are investigated and compared in terms of radio-electrical performances.

Regarding the constraints in terms of dimensions limitation, as well as the radiating element location that affects the impedance matching, the antenna is expanded by folding it at its extremity, to ensure on one hand a resonance at the ISM band, and on another hand a good size optimization and mechanical rigidity.

**Figure 23. Metallic inverted F antenna configuration: (a) simplified model (b) complete model**

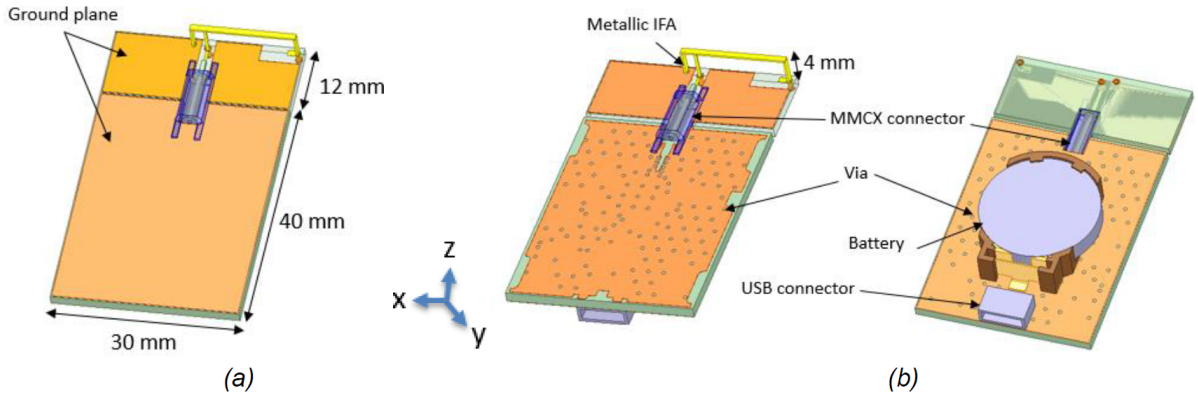


### 3.6.2 Simulation results

The simulated return loss against frequency is as represented in Figure 24. The agreement between basic and complete model is good. The antenna is well matched to 50 Ω impedance and provides a return loss of -13 dB at 2.45 GHz.

Figure 25 illustrates the variation of the input impedance versus frequency. Good stability can be noticed for the real and imaginary parts except for the maximum points for which a small decrease for the complete model is observed.

**Figure 24. Simulated return loss versus frequency for simple and complete models**

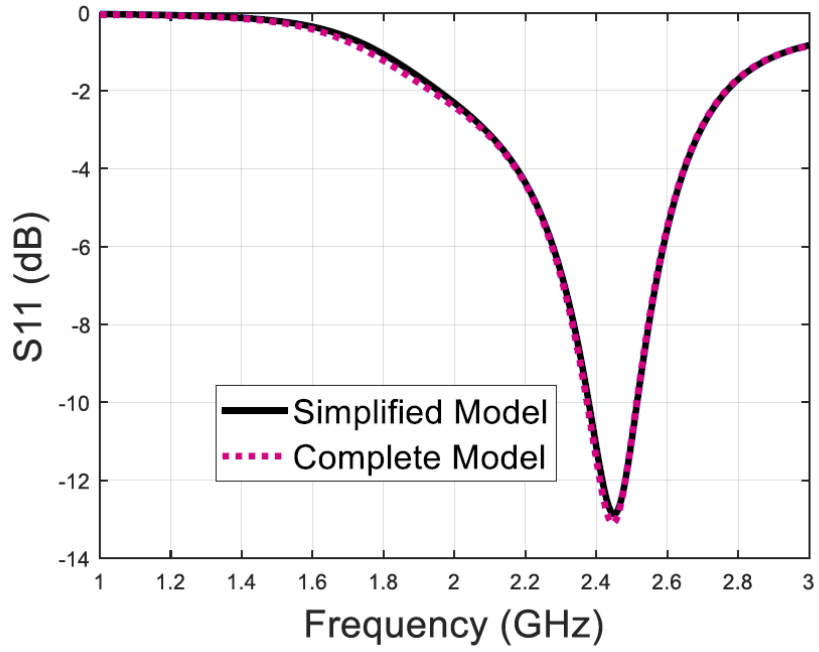

Figure 25. **Simulated input impedance versus frequency for simple and complete models**

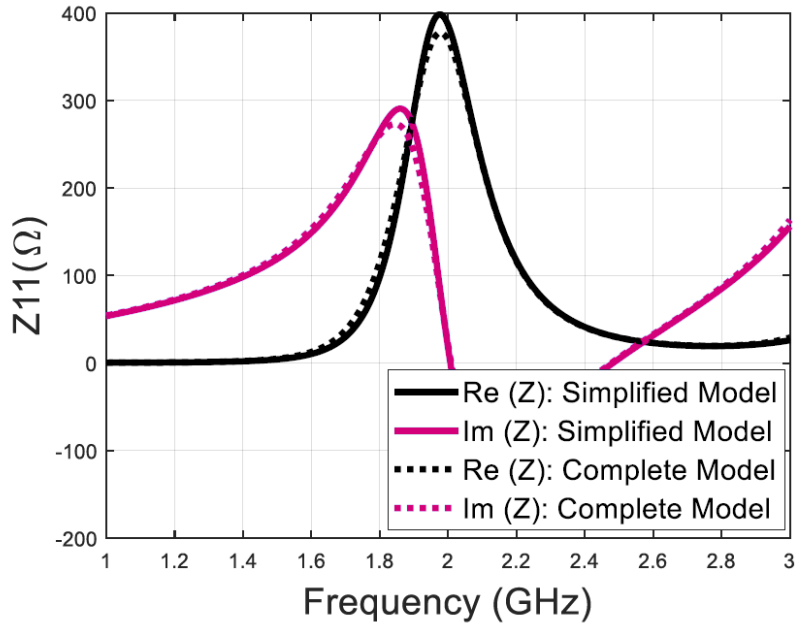


Figure 26 presents the impact of the context (complete model) on the antenna efficiency. A small peak efficiency drop of approximately 1 % is noticeable, but this remains largely acceptable.

Figure 27 exposes the variation of the 2D radiation pattern following the three principal planes at 2.45 GHz. Omnidirectional comportment is perceived following Θ=90° plane, while a quasi-broadside one is observed in φ=0° plane. The radiation appears less symmetrical in the φ=0° and φ=90° cut planes compared to the printed IFA.

Figure 26. **Simulated efficiency versus frequency for simple and complete models**